Biochimica et Biophysica Acta 1777 (2008) 514–524

Contents lists available at ScienceDirect

Biochimica et Biophysica Acta

journal homepage: www.elsevier.com/locate/bbabio

Distinct organization of energy metabolism in HL-1 cardiac cell line and cardiomyocytes

Margus Eimre [a], Kalju Paju [a], Sophie Pelloux [b], Nathalie Beraud [c], Mart Roosimaa [a], Lumme Kadaja [a], Marju Gruno [a], Nadezhda Peet [a], Ehte Orlova [a], Reele Remmelkoor [a], Andres Piirsoo [a], Valdur Saks [c,d], Enn Seppet [a,*,1]

[a] Department of Pathophysiology, Centre of Molecular and Clinical Medicine, Faculty of Medicine, University of Tartu, Tartu, Estonia
[b] Laboratory of Cardioprotection, INSERM U886, Univ Lyon1, Lyon F-69008, France
[c] Laboratory of Fundamental and Applied Bioenergetics, INSERM U884, Joseph Fourier University, Grenoble, France
[d] Laboratory of Bioenergetics, National Institute of Chemical Physics and Biophysics, Tallinn, Estonia

ARTICLE INFO

Article history:
Received 26 January 2008
Received in revised form 15 March 2008
Accepted 18 March 2008
Available online 29 March 2008

Keywords:
HL-1 cell
Heart
Energy transfer
Kinase
Gene expression

ABSTRACT

Expression and function of creatine kinase (CK), adenylate kinase (AK) and hexokinase (HK) isoforms in relation to their roles in regulation of oxidative phosphorylation (OXPHOS) and intracellular energy transfer were assessed in beating (B) and non-beating (NB) cardiac HL-1 cell lines and adult rat cardiomyocytes or myocardium. In both types of HL-1 cells, the *AK2*, *CKB*, *HK1* and *HK2* genes were expressed at higher levels than the *CKM*, *CKMT2* and *AK1* genes. Contrary to the saponin-permeabilized cardiomyocytes the OXPHOS was coupled to mitochondrial AK and HK but not to mitochondrial CK, and neither direct transfer of adenine nucleotides between CaMgATPases and mitochondria nor functional coupling between CK-MM and CaMgATPases was observed in permeabilized HL-1 cells. The HL-1 cells also exhibited deficient complex I of the respiratory chain. In conclusion, contrary to cardiomyocytes where mitochondria and CaMgATPases are organized into tight complexes which ensure effective energy transfer and feedback signaling between these structures via specialized pathways mediated by CK and AK isoforms and direct adenine nucleotide channeling, these complexes do not exist in HL-1 cells due to less organized energy metabolism.

1. Introduction

The mitochondria in the cardiomyocytes are regularly arranged within the limits of the sarcomeres in a longitudinal lattice between the myofibrils [1,2]. After permeabilization of cardiomyocytes with saponin the mitochondria exhibit much higher apparent Km values for exogenous ADP in regulation of respiration than the isolated mitochondria. Thus, mitochondrial function is differently regulated in vivo, when these organelles can interact with other intracellular structures (e.g. sarcomeres, sarcolemma, etc) compared to conditions in vitro, when the normal intracellular interactions are lost [3,4]. In the same studies, it was revealed that compared to mitochondria in cardiac cells, the Km for ADP is always significantly lower in white glycolytic muscle fibers, practically equaling to its level in isolated muscles. So it became clear that the regulation of mitochondrial function depends also on the muscle type, probably due to a different localization of mitochondria within the cellular structure in oxidative and glycolytic muscle cells [3,4]. Indeed, the importance of structural factors in controlling mitochondrial function was confirmed by observations that modification of cell structure by treating permeabilized cardiomyocytes with minute concentrations of proteolytic enzymes [5] or by causing contracture with excess Ca^{2+} [6] decreases the Km for ADP to the levels close to those registered in isolated mitochondrial fractions or glycolytic muscles. That these changes may be related to alterations in cytoskeletal proteins was revealed by an observation that mitochondrial affinity to exogenous ADP is higher in permeabilized cardiomyocytes obtained from desmin- and dystrophin-deficient mice than in cells from wild-type counterparts [7,8]. Altogether these findings have led us to the hypothesis that in cardiac cells the mitochondria and ATPases, with participation of cytoskeletal proteins, form complexes, termed as intracellular energy units (ICEUs) [5,9,10]. Owing to the local diffusion restrictions within the ICEUs [11] these complexes separate part of cellular adenine nucleotides from the bulk phase of cytoplasm and, on the other hand, are not easily permeable for exogenously added adenine nucleotides that gives rise to high apparent Km for ADP in regulation of respiration. Inside the ICEUs, the specialized pathways mediated by CK, AK, and direct adenine nucleotide channeling ensure energy transfer and feedback between mitochondria and ATPases [5,9,10].

To further address the role of structure–function relationships in establishing the control over mitochondrial function, we have taken

* Corresponding author. Department of Pathophysiology, Faculty of Medicine, University of Tartu, 19 Ravila Street, 50411 Tartu, Estonia. Tel.: +372 7374371; fax: +372 7374372.
E-mail address: enn.seppet@ut.ee (E. Seppet).
[1] Current temporary address (until April 6, 2008): KeyNeurotek Pharmaceuticals AG, ZENIT Technology Park, Leipziger Str. 44, D-39120, Magdeburg, Germany. Tel.: +49 372 5117126; fax: +49 391 611 7221.

0005-2728/$ – see front matter © 2008 Elsevier B.V. All rights reserved.
doi:10.1016/j.bbabio.2008.03.019

advantage of HL-1 cell line as a model of cardiac cells with distinct structural and functional properties compared to normal cardiomyocytes [12]. This cell line, first developed by Claycomb et al. [13], can continuously divide and spontaneously contract (beating (B) HL-1 cells) while maintaining a differentiated cardiac phenotype through indefinite passages in culture [13,14]. Recently, a novel subtype of HL-1 cells, the non-beating (NB) cells, was developed by culturing B HL-1 cells in the medium with specific serum that caused the cells to stop beating without hindering their proliferation in normal culture medium [15]. Differently from the original B HL-1 cells, the NB HL-1 cells do not present the pacemaker current, spontaneous depolarization or calcium oscillations [15]. Confocal imaging of mitochondria revealed very different structural organization of the HL-1 cells as compared to adult cardiomyocytes. In contrast to the perfect crystal-like intracellular arrangement of mitochondria in adult cardiomyocytes, these organelles are rather chaotically situated in HL-1 cells, presenting filamentous and dynamically changing pattern [13–15]. Whereas the B HL-1 cells possess some residual sarcomeres, the NB HL-1 cells are devoid of these structures [13–15]. Based on these characteristics we have assumed that if the localization of mitochondria strictly near sarcomeres is indeed a prerequisite for formation and function of ICEUs, these complexes should not exist in HL-1 cells, which means that mitochondrial OXPHOS should also be regulated differently in these cells as compared to adult cardiac cells. In support of this assumption we have found that in both B and NB HL-1 cells permeabilized by saponin, the mitochondria exhibited very low apparent Km for exogenous ADP in stimulation of respiration as compared to that in adult cardiomyocytes [12]. Moreover, in NB HL-1 cells creatine was unable to stimulate respiration, indicating the absence of functional coupling between mitochondrial CK (mi-CK) and adenine nucleotide translocase (ANT) [12]. These findings suggest that diffusion of ADP is not significantly restricted and CK-mediated system of energy transfer may not function in HL-1 cells. Hence, energy metabolism in HL-1 cells might be organized differently from that observed in adult cardiac cells. At present, however, nothing is known regarding the expression of the kinases participating in the intracellular energy transfer systems in HL-1 cells. Therefore, the purpose of this study was to characterize the expression of CK, AK and HK in relation to their impact on mitochondrial or ATPase functions. The preliminary results of this study have been partially published in abstract form [16].

2. Materials and methods

2.1. Laboratory animals

Adult male outbred Wistar rats weighing 300–350 g or mice (25–35 g) were used in the experiments. The animals were kept, fed and studied in accordance to the Guide for the Care and Use of the Laboratory Animals (NIH publication no. 85-23, revised 1996).

2.2. Preparation of isolated cardiomyocytes, cardiac fibers and HL-1 cell culture

The cardiomyocytes and cardiac fibers from adult rat ventricular myocardium were isolated and permeabilized by incubating for 30 min at 4 °C with 50 μg/ml saponin as described previously [9,10,17]. The B and NB HL-1 cells were cultured as described before [15]. The cells were detached by trypsinization and the cell's suspension was washed 4 times and centrifuged for 5 min at 1000 rpm with phosphate-buffered saline (PBS) at 4 °C. Subsequently, the sediment was resuspended in Mitomed medium (see Section 2.4) and used in the experiments.

2.3. Electron and confocal microscopy

Cells were fixed for 1 h at 4 °C in 2.5% glutaraldehyde in a cacodylate buffer (pH 7.4). Fixed cells were then centrifuged at 300 *g* for 5 min. After washing the cells in the pellet were postfixed in 2% osmium tetraoxide for 1 h. The samples were dehydrated in graded alcohol and embedded in Epon 812. The ultrathin sections were stained with lead citrate and uranyl acetate and studied under transmission electron microscope Tecnai 10 (FEI, Netherlands). For confocal microscopy, cells were detached by trypsin incubation and washed with Mitomed solution 5 times. Then the cells were incubated with a mitochondria specific dye, MitoTracker Green FM (excitation 488 nm, emission 516 nm) which becomes fluorescent accumulating in lipid environment of mitochondria and is insensitive to membrane potential and a nucleus dye, Hoechst 342 (emission 350 nm, excitation 461 nm) which is cell permeable nucleic acid stain (DNA bound). The digital images of MitoTracker® and Hoechst 342 fluorescence were acquired with an inverted confocal microscope (Leica DM IRE2) with a 63-× water immersion lens. The MitoTracker® Green fluorescence was excited with the 488 nm line of argon laser, using 510 to 550 nm for emission.

2.4. Measurement of mitochondrial respiration

The rates of oxygen uptake were recorded using a high-resolution Oroboros oxygraph (Paar KG, Austria) equipped with a Clark oxygen sensor. The HL-1 cells or permeabilized cardiac fibers/cardiomyocytes were incubated in an oxygraph chamber in the modified Mitomed solution [12,17,18] of the following composition: 110 mM sucrose, 60 mM K-lactobionate, 0.138 mM CaK_2EGTA, 0.362 mM K_2EGTA, 3 mM $MgCl_2$, 0.5 mM dithiothreitol, 20 mM taurine, 3 mM KH_2PO4, 20 mM K-HEPES, pH 7.1, with 1 mg/ml essentially fatty acid free bovine serum albumin (BSA). The free $[Ca^{2+}]$ in this solution was 0.2 μM as detected fluorimetrically (FlexStation II, Molecular Devices Corporation, USA) by using the Ca^{2+} calibration buffer kit and indicator fura 4F (Molecular Probes Europe BV, Leiden, Netherlands). Where required, ATP or ADP were added together with $MgCl_2$ (0.8 mol/mol for ATP and 0.6 mol/mol for ADP) to keep free Mg^{2+} constant in the medium.

For permeabilization of the cell membrane, 50 μg/ml saponin was added and the cells were incubated during the 15 min. In preliminary experiments it was found that the 15 min incubation with saponin was sufficient to permeabilize the cells because during that period a gradual increase in ADP-stimulated respiration up to maximal steady state level was observed. Then the analysis of the function of the respiratory chain was started by adding 10 mM glutamate and 2 mM malate. After the registration of basal respiration rate in non-phosphorylating conditions (V_0), 2 mM MgADP was added to monitor the maximum rate of NADH-linked state 3 respiration (V_{Glut}), followed by successive additions of 10 μM rotenone to inhibit the complex I, 10 mM succinate to activate $FADH_2$-linked state 3 respiration (V_{Succ}), 0.1 mM atractyloside to assess respiratory control by blocking ANT (V_{Atr}), 10 μM antimycin A to inhibit the electron flow from complex II to cytochrome *c* (V_{Ant}), 0.5 mM TMPD with 2 mM ascorbate to activate cytochrome oxidase (COX), 8 μM cytochrome *c* to monitor whether it limits the respiration rate, and 5 mM NaN_3 to quantify COX activity as a NaN_3-sensitive portion of respiration (V_{COX}). A difference between the respiration rates in the presence of atractyloside and antimycin A ($V_{Atr}-V_{Ant}$) was taken to measure the proton leak.

A coupling between OXPHOS and mitochondrial CK (mi-CK) was estimated by using two protocols. In the first one, the HL-1 cells were incubated for 15 min in Mitomed medium at 25 °C in the presence of 50 μg/ml saponin, 10 mM succinate and 10 μM rotenone, and the basal rate of respiration (V_0) was registered. Thereafter 0.1 mM MgATP was added to achieve a submaximal flux of endogenous ADP produced by CaMgATPases to stimulate the respiration, 2 mM AMP was added to monitor the effect of ADP produced by mitochondrial AK2, 0.2 mM diadenosine pentaphosphate (AP_5A) was added to inhibit the AK activity, and 20 mM creatine was added to activate mi-CK. The experiment was continued by adding 2 mM MgADP to gain the maximum rate of OXPHOS, followed by the addition of 0.1 mM atractyloside to monitor the respiratory control via ANT. Then 200 nM FCCP was added to register the maximum uncoupled respiration and 8 μM cytochrome *c* was added to assess the intactness of the mitochondrial outer membrane (MOM). In the second protocol, after registration of V_0 in the presence of 5 mM PEP, 2 mM MgATP, 20 IU/ml PK and 20 mM creatine were successively added. The same protocol was applied to estimate the coupling between mitochondrial AK2 (mi-AK2) and OXPHOS, except that 20 mM creatine was replaced by 2 mM AMP. To assess the role of HK in stimulating OXPHOS the cells were permeabilized as described above and incubated in the presence of 0.1 μM MgATP. Then 10 mM glucose was added followed by additions of 2 mM MgADP and 0.1 mM atractyloside. In separate experiments, the role of HK bound to mitochondria was analyzed after the washout of the cytoplasmic enzymes. For this purpose, the cells were incubated in shaking conditions in 3 ml Mitomed solution with 50 μg/ml saponin for 10 min at room temperature and centrifuged at 1000 rpm for 5 min. Then the supernatant was removed, and the pellet was resuspended in Mitomed and centrifuged 1000 rpm 5 min, this washing step was repeated twice more, and the final pellet was resuspended in Mitomed and used for experiments as a stock solution. To assess the function of HK, the cells were incubated in oxygraph chamber without saponin and the experiments were started with addition of 0.1 mM MgATP as described above.

2.5. Determination of the flux of ADP produced in ATPase reactions

The suspension of HL-1 cells (10–30 μl) was incubated in the spectrophotometric (Perkin-Elmer Lambda 900) cuvette containing Mitomed supplemented with 5 mM PEP, 20 IU/ml PK, 20 IU/ml LDH and 0.24 mM NADH at 25 °C. The medium was continuously mixed with a magnetic stirrer operated by the Variomag Telemodul (H+P Labortechnic, Germany). To permeabilize the cells, 50 μg/ml saponin was added and the cells were incubated for 15 min before the following successive additions were made: 1 mM MgATP, 10 mM glutamate and 2 mM malate (or 10 mM succinate with 10 μMrotenone), and 0.1 mM atractyloside. The extent of mitochondrial rephosphorylation of ADP produced in the CaMgATPase reactions was quantified as the flux through the PEP-PK system registered by the changes in NADH concentration at 340 nm decreased after switching on the OXPHOS by adding respiratory substrates. A coupling of cytosolic CK isoforms to CaMgATPases was assessed from the decrease of the ADP flux through the PK-PEP system caused by 20 mM phosphocreatine (PCr) added after stabilization of the ADP flux in the presence of atractyloside.

2.6. ATP and lactate/glucose ratio measurements

For ATP measurements in cell lysates, the NB HL-1 cells were first incubated for 10 min in Tyrode's solution containing 150 mM NaCl, 5.4 mM KCl, 0.9 mM NaH_2PO_4, 1.8 mM $CaCl_2$, 1.2 mM $MgCl_2$, 10 mM HEPES, pH 7.2, buffered with NaOH. This solution also contained 10 mM glucose for control condition, or no glucose and 2 mM 2-deoxyglucose to inhibit glycolysis. Then the cell plates were plunged into boiling water for 1.5 min, detergent solution was added (25 mM Tris, 2 mM EDTA, 0.5 mM DTT, 1/1000 Tween, pH 7.75 with acetic acid) and the plates were set to freeze at −80 °C. Then the cells were thawed, sonicated, and scraped off on ice. The cell extracts were pipetted into pre-cooled tubes, spinned down at 13 000 rpm for 15 min at +4 °C. The ATP concentration was measured in supernatants using Prolux luciferase-luciferin kit (Euralam, France) in a luminometer (Optocomp, MGM Instruments Inc., Hamden, CT, USA). For measurements of lactate/glucose ratio, supernatants from 25 cm^2 culture flasks of NB HL-1 (10^7 cells) were kept after 24, 48 and 72 h of culture in normal culture medium (Supplemented Claycomb Medium) containing 21 mM glucose and 2 mM lactate. Glucose and lactate concentrations were determined using glucose-sensitive and lactate-sensitive electrodes (CCX Analyser, Nova Biomedical, Waltham, MA, USA). Glucose consumption and lactate production were calculated from the differences between their concentrations in samples and control medium.

2.7. Determination of the activities of kinases

Rat ventricular myocardial or HL-1 cells were homogenized by sonication (Bandelin Sonopuls HD 2200, probe MS 72) in ice-cold PBS. The homogenates were incubated in a spectrophotometric cuvette in stirring conditions in the Mitomed medium supplemented with NADH 0.24 mM, PEP 0.8 mM, 6 IU/ml PK, and 3 IU/ml LDH (pH 7.1, 25 °C). After registration of basal CaMgATPase in the presence of 1 mM MgATP, 1.3 mM AMP was added to determine the AK activity from the changes in NADH oxidation rates at 340 nm. For CK total activity measurements the Mitomed medium was supplemented with 2 mM MgADP, 6 mM glucose, 0.6 mM NADP, 0.5 mM AP_5A, 2 IU/ml hexokinase (HK), and 2 IU/ml glucose-6-phosphate dehydrogenase (G6PDH) at 25 °C. Then the specimen was added, and after stabilizing the optical density, the reaction was started by addition of 20 mM PCr and the rate of NADPH formation was registered. The HK activity was measured in Mitomed medium in the presence of 2 mM MgATP, 0.6 mM NADP and 2 IU/ml G6PDH, and the rate of NADPH formation was monitored spectrophotometrically (Perkin-Elmer Lambda 900) after addition of 10 mM glucose at 340 nm, 25 °C. To measure the mitochondria-bound HK activity in HL-1 cells, the cells were permeabilized with saponin (50 μg/ml, 10 min at room temperature) in the Mitomed solution as described above (Section 2.4) before assessment.

2.8. Determination of isoform profile of kinases

The HL-1 cells frozen at −80 °C were thawed at 0 °C and homogenized in the medium containing: 1 mM EGTA, 1 mM dithiothreitol, 2 mM $MgCl_2$, 5 mM HEPES and 1% Triton X-100 (1:20 w/v), pH 8.7, by ultrasound on ice during 15 s followed by a 1 min period of keeping the probe on ice. Then the same cycles were repeated thrice, and the homogenates were left on ice for 1 h for complete extraction of the CK. The CK isoform profile was assayed as follows. Samples of 4 μl (20–40 μg protein, 0.002–0.004 IU CK) of homogenates were applied to a 1% agarose gel and subjected to electrophoresis for 1 h at 180 V in Tris/barbital buffer (50 mM, pH 8.9). To reveal the CK isoenzyme activities the gel was incubated with a staining solution-soaked paper for 30 min at 30 °C, and the fluorescence of the produced NADPH was visualized under UV light and analyzed with Fluor-S Multi-imager (Bio-Rad, USA). The staining solution contained 22 mM MES (pH 6.8), 50 mM magnesium acetate, 70 mM glucose, 120 mM *N*-acetyl cysteine, 130 mM PCr, 9 mM ADP, 10 mM NADP, 18 mM AMP, 0.75 mM AP_5A, 18 U/ml HK, and 6 U/ml G6PDH. Electrophoresis of HK was performed in 1% agarose gel in Tris/barbital buffer (50 mM, pH 8.5, 180 V) at 4 °C. Then the gels were incubated with paper soaked in staining solution (100 mM glucose, 50 mM magnesium acetate, 22 mM MES, 120 mM *N*-acetyl cysteine, 10 mM NADP, 50 mM ATP, and 6 U/ml G6PDH, pH 6.8) for 60 min at 37 °C and visualized under UV light.

2.9. SDS-polyacrylamide gel electrophoresis and immunoblotting

Fifty micrograms of total protein in homogenates was separated by standard 12% SDS-polyacrylamide gel electrophoresis and electrotransferred by semidry blotting (Hoefel Pharmacia Biotech Inc. San Fransisco CA, USA) on a nitrocellulose membrane (Shleicher & Schüell, Dassel, Germany) according to the manufacturer's instructions. The membranes were blocked with 4% fat-free milk powder in T-TBS (20 mM Tris–HCl pH 7.5, 150 mM NaCl, 0.05% Tween 20) overnight at 4 °C, incubated for 15 min at room temperature and washed for 4×5 min with T-TBS. Then the membranes were incubated for 1 h with ubiquitous mitochondrial CK rabbit immune sera (1:2000 dilution in a blocking buffer) or with affinity-purifed chicken anti-B-CK IgY (1:500 dilution in a blocking buffer) at room temperature [19]. For detecting AKs, the membranes were incubated for 1 h at room temperature with rabbit polyclonal antibodies against AK1 (H-90, Santa Cruz Biotechnology, Inc., USA) or AK2 (H-65, Santa Cruz Biotechnology, Inc., USA) (dilution 1:500 in a blocking buffer), washed for 4×5 min in T-TBS and incubated for 1 h with the peroxidase-coupled secondary antibody, either goat anti-rabbit IgG (Nordic, Lausanne, Switzerland) (1:1000 dilution in a blocking buffer) or rabbit anti-chicken IgY (Jackson ImmunoResearch, West Grove, PA) (1:3000 dilution in a blocking buffer) and finally washed for 4×5 min with T-TBS. The blots were developed with the enhanced chemiluminescence substrate (Amersham, Buckinghamshire, UK) and exposed to an X-ray film.

2.10. RNA isolation

Total RNA from $1\cdot10^6$–$1\cdot10^7$ frozen HL1 cells suspended in PBS was isolated using the RNeasy Mini Kit according to the manufacturer's protocol (Qiagen, Hilden, Germany). The integrity of RNA was verified by 0.8% agarose gel electrophoresis. Ribosomal RNA bands 28 S and 18S were visualized by ethidium bromide staining. Quantification of the nucleic acid was carried out spectrophotometrically (Lambda 900, Perkin-Elmer) at 260 nm, and the purity of RNA preparation was checked by assessing the *A*260/*A*280 ratio. Thereafter the gel was *trans*-illuminated with UV light and photographed by Syngene Gel Documentation System with a Syngene Software GeneSnap (Syngene, UK).

2.11. Reverse transcriptase reaction

For reverse transcription (RT), total RNA (approximately 500 ng) obtained from HL-1 cells was processed for single-stranded cDNA synthesis using Superscript III reverse transcriptase (Invitrogen, Karsruhe, Germany) and oligo dT (Proligo France SAS, Paris, France). All RT reactions were done in a PCR thermocycler GeneAmp® PCR System 2400 (Perkin-Elmer/Applied Biosystems). The resulting cDNA was used for real-time RT-PCR.

2.12. Relative quantification of mRNA expression by real-time RT-PCR

The real-time RT-PCR was performed by an ABI PRISM 7000 Sequence Detection System (Perkin-Elmer/Applied Biosystems) using the QuantiTect SYBR Green PCR Kit (Qiagen, Hilden, Germany). The samples in the reaction mixture, supplied with QuantiTect SYBR Green PCR Kit as well as no template controls, were loaded in a total volume of 31 μl per reaction. Thereafter gene specific primers were added into the reaction mix in the concentration of 0.3 μM. The oligonucleotide primers (Proligo France SAS, Paris, France) used for real-time PCR analysis are shown in Table 1. An identical PCR cycle profile was used for all genes. The amplification started by heat activation of HotStarTaq® DNA polymerase at 95 °C for 15 min. The following 35 cycles of PCR consisted of denaturation step for 15 s at 94 °C, primer annealing step for 30 s at 59 °C and for 30 s extension phase at 72 °C. The expression data were analyzed by using a comparative critical threshold method, where the amount of the gene of interest was normalized to the housekeeping gene (hypoxanthine ribosyl transferase (HPRT1) and expressed relative to the mean values of calibrator samples using the following equation [20]:

$$\text{Fold induction} = 2^{-\Delta\Delta CT} \quad (1)$$

where ΔΔ*C*T equals to the threshold cycle difference of the gene of interest relative to reference gene HPRT1 in an unknown sample minus the threshold cycle difference of the unknown gene relative to reference gene HPRT1 in calibrator sample (adult rodent heart). The amplified cDNAs were separated in a 1.7% agarose gel to verify amplicons by size using DNA size marker (100 bp Generuler, Fermentas, Lithuania).

2.13. Statistical analysis

The means ± SEM are presented. Statistical analysis of data was performed by one-way ANOVA with Bonferroni or Dunnett's post test and by Mann–Whitney test using GraphPad Prism version 5.00 for Windows.

Table 1
Primer design for real-time PCR analysis

Primer	Sequences 5′>3′	Amplicon length, bp
CKM F	GTCCGTGGAAGCTCTCAACAG	133
CKM R	CAGAGGTGACACGGGCTTGT	
CKB F	TCGTGGCATATGGCACAATG	114
CKB R	CGGGTGAACACTTCCTTCATG	
CKMT2 F	AGCAAGGATCCACGCTTTTCT	126
CKMT2 R	TCTGCCGATCCGATCTATGTT	
AK1 F	CCAATGGCTTCCTGATCGA	84
AK1 R	GCAGTGTGGGCTGTCCAAT	
AK2 F	GGCAGGCTGAAATGCTTGA	92
AK2 R	GATCAGCAGCGAGTCTTGGAT	
HK1 F	CACCGGCAGATTGAGGAAAC	100
HK1 R	CTCAGCCCCATTTCCATCTCT	
HK2 F	GGAACCCAGCTGTTTGACCA	87
HK2 R	CAGGGGAACGAGAAGGTGAAA	
HPRT1 F	GCAGTACAGCCCCAAAATGG	85
HPRT1 R	AACAAAGTCTGGCCTGTATCCAA	

Expression of HK3 was analyzed using Mm HK3 Quantitect Primer Assay (Qiagen) that produces amplicon length of 111 bp or RT^2 PCR Primer Set for Mouse HK3 (Super Array BioScience Corporation, USA) that produces amplicon length of 98 bp.

3. Results

3.1. Peculiarities of the respiratory chain and oxidative phosphorylation in HL-1 cells

Fig. 1 demonstrates that in the solution the HL-1 cells acquired a rounded shape, a typical feature seen after the detachment of cells by trypsinization. Confocal microscopic studies of non-fixed HL-1 cells before saponin treatment (Fig. 1A, B) showed the presence of both granular and fibrilar forms of the mitochondria arranged chaotically, in contrast to the crystal-like organization of mitochondria in cardiomyocytes [1]. Electron microscopy (Fig. 1C, D) revealed focal impairment or loss of the sarcolemmal structure after treatment with saponin. Notably, the mitochondria in the cells exhibited some swelling but intact membranes, and all of them remained within the cell interior despite marked deterioration of the cell membrane. Thus, the 15 min treatment of cells with saponin was optimal for selective permeabilization of the sarcolemma without total disintegration of the cell structure and translocation of mitochondria into the medium.

Fig. 2 and Table 2 show that mitochondrial respiration in permeabilized HL-1 cells substantially increased over the basal levels after addition of MgADP and that this ADP-dependent activation was effectively abrogated with atractyloside. Hence, the mitochondrial inner membrane was intact ensuring effective control over OXPHOS by ANT. Addition of cytochrome *c* to cells in conditions of maximum activation of COX (Fig. 2) or uncoupled respiration (Fig. 6A) did not increase the respiration which means that the mitochondria had not

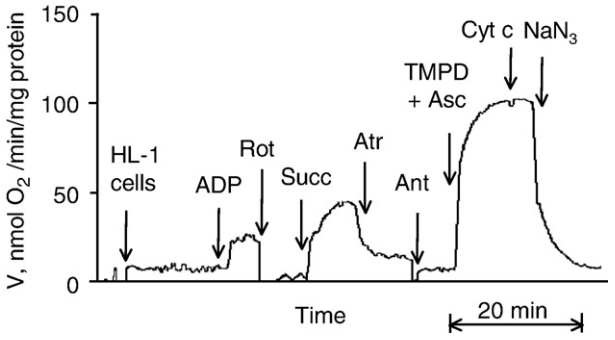

Fig. 2. Original recording of the assessment of the respiratory chain function in B HL-1 cells. HL-1 cells — HL-1 cells incubated for 15 min in Mitomed medium at 25 °C in the presence of 50 μg/ml saponin. Further additions: ADP — 2 mM MgADP, Rot — 10 μM rotenone, Succ — 10 mM succinate, Atr — 0.1 mM atractyloside, Ant — 10 μM antimycin A, TMPD+Asc — 0.5 mM TMPD with 2 mM ascorbate, Cyt *c* — 8 μM cytochrome *c*, and NaN_3 — 5 mM NaN_3.

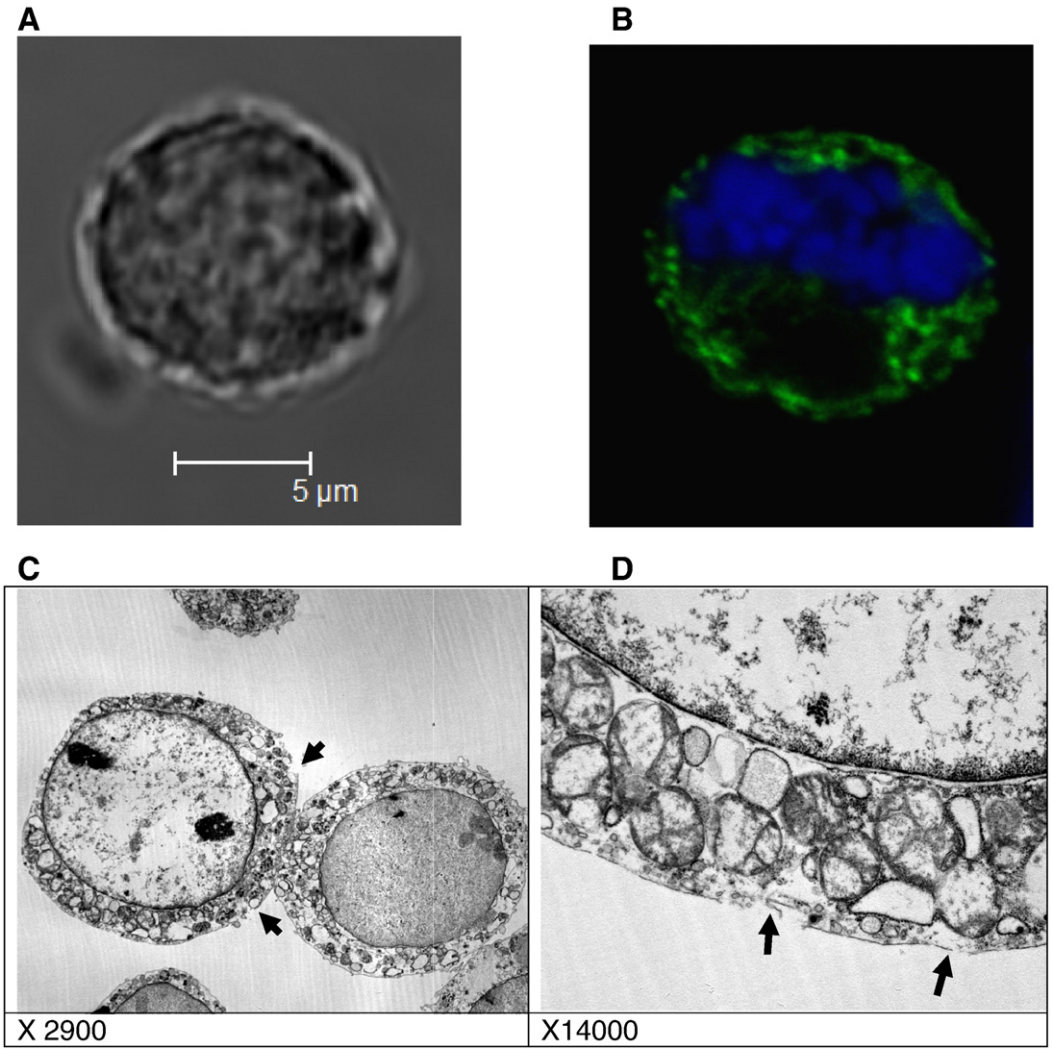

Fig. 1. A and B. Confocal images of the detached HL-1 NB cells in Mitomed medium. A. Transmission image; B. Visualization of mitochondria and nucleus. C and D. Electron micrographs of the B HL-1 cells after detachment and 15 min treatment with 50 μg/ml saponin followed by thrice washout (see Materials and methods). C. Magnification ×2900, D. Magnification ×14,000. The arrows point to focal impairment of the cell membrane.

Table 2
Characterization of the respiratory chain in beating and non-beating HL-1 cells

Parameter of oxidative phosphorylation	Type of HL-1 cells	
	Non-beating	Beating
	$n=4$	$n=5$
V_0	7.64±1.25	6.8±0.80
V_{Glut}	20±3.41	20.1±3.65
RCI_{Glut}	2.73±0.50	2.95±0.44
V_{Succ}	49.07±5.74$^{\#}$	44.8±2.66$^{\#}$
V_{Atr}	16.2±0.62	12.2±1.37
$V_{Atr}-V_{Ant}$	9.14±1.11	6.77±0.72
RCI_{Succ}	3.01±0.27	3.85±0.47
V_{Glut}/V_{Succ}	0.403±0.043	0.442±0.071
V_{COX}	98.85±12.36	114.0±7.87
V_{Glut}/V_{COX}	0.20±0.02	0.18±0.04
V_{Succ}/V_{COX}	0.50±0.01$^{¤}$	0.39±0.03*$^{¤}$

The rates of respiration (V) are given in nmol O_2/min/mg protein. V_0 — basal respiration without ADP or ATP; V_{Glut} — ADP-stimulated respiration in the presence of glutamate and malate; RCI_{Glut} — respiration control index calculated as V_{Glut}/V_0; V_{Succ} — ADP-stimulated respiration in the presence of rotenone and succinate; V_{Atr} — respiration after inhibition of succinate-stimulated respiration by atractyloside; $V_{Atr}-V_{Ant}$ — difference between the respiration rates with atractyloside and antimycin A which is equivalent to proton leak. RCI_{Succ} — V_{Succ}/V_{Atr}; V_{COX} — the respiratory equivalent of cytochrome oxidase activity calculated as $[V_{COX}=V_{TMPD}-V_{TMPD+NaN_3}]$ where V_{TMPD} and $V_{TMPD+NaN_3}$ are TMPD-stimulated respiration rates before and after addition of NaN_3. * — $p<0.05$ compared to NB HL-1 cells. $^{\#}$ — $p<0.001$–0.05 compared to V_{Glut}. $^{¤}$ — $p<0.001$–0.0001 compared to V_{Glut}/V_{COX}.

lost cytochrome *c* from their intermembrane space. In line with morphological analysis (Fig. 1) these observations suggest that saponin treatment resulted in permeabilization of sarcolemma allowing MgADP to reach mitochondria but did not destroy the mitochondrial membranes in HL-1 cells.

Notably, the functional activity of COX markedly exceeded that for upstream complex I or complex II expressed as V_{Glut} and V_{Succ} (Fig. 2, Table 2). The V_{Succ}/V_{COX} was higher than V_{Glut}/V_{COX}, and the V_{Glut}/V_{Succ} was about 0.4–0.44 which is less than observed in the mitochondria in normal myocardium (1.2–1.3 [10]). These data indicate a relative deficiency of the complex I of the respiratory chain [21,22]. In general, the mitochondria appeared to be similar in B and NB HL-1 cells, except that the latter exhibited higher V_{Succ}/V_{COX} than the former (Table 2).

3.2. Differences in energy transfer pathways between cardiomyocytes and HL-1 cells

Fig. 3 demonstrates that the total activity of CK in the homogenates of HL-1 cells equaled to that of total ATPase. It should be considered here that because the Mitomed medium contained both Mg^{2+} and Ca^{2+} ions, this ATPase activity actually represents a sum of all Ca^{2+}- or Mg^{2+}-activated ATPases and therefore can be termed as CaMgATPase. However, the CK activity was about 30 times lower than in the homogenates of rat myocardium (5284±978 nmol/min/mg protein) that is in conformity with earlier data [3,12,23]. The total AK activity was about five-fold higher than CK activity. Such AK to CK activity ratio in HL-1 cells contrasts to that in cardiomyocytes where the CK activity normally prevails against AK [24]. The HL-1 cells also exhibited much higher HK activity (150–170 nmol/min/mg protein) compared to adult rat cardiomyocytes or intact myocardium (30–40 nmol/min/mg protein). Akin to respiratory properties, the B and NB cells exhibited no differences in total enzyme activities.

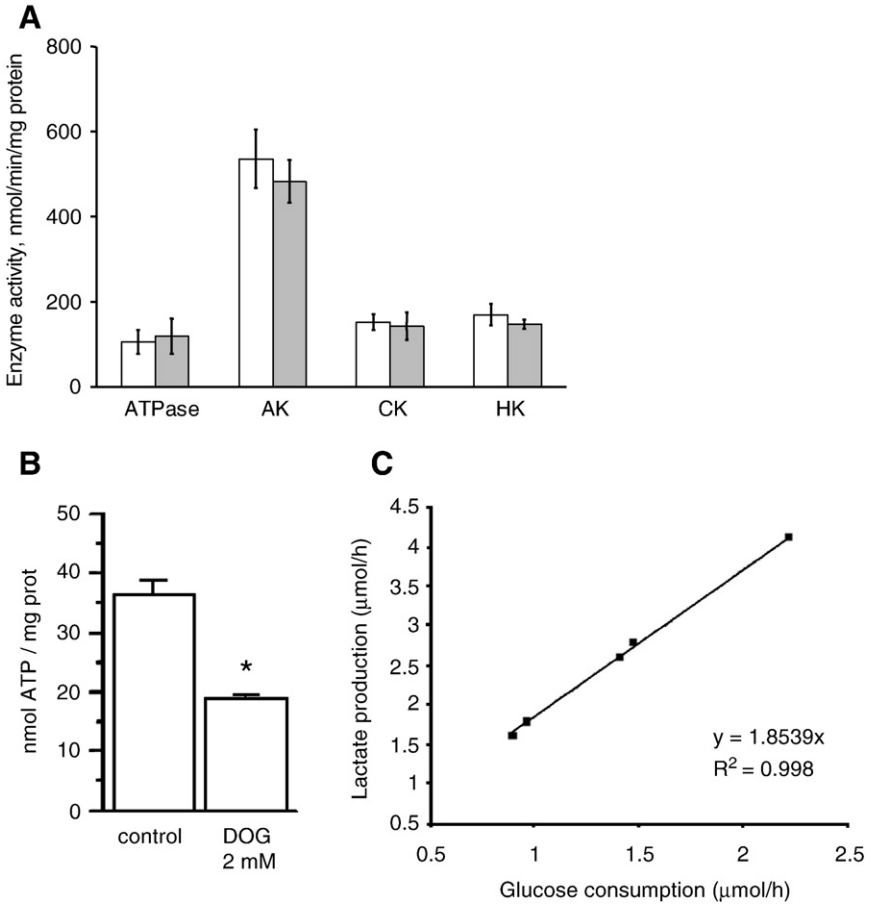

Fig. 3. A. Total activities of CK, AK and HK in HL-1 NB (white columns, $n=6$) and B HL-1 cells (grey columns, $n=8$). B. Global ATP measurement in NB HL-1 cells. ATP concentration in the cell extracts from NB HL-1 cells was determined after 10 min without glucose and with 2-deoxyglucose (DOG) versus control solution containing 10 mM glucose. * — $p<0.01$ versus control. C. Lactate/glucose ratio represented by the slope of correlation between lactate production and absolute value of glucose consumption in NB HL-1 cells.

Fig. 3B shows that HL-1 cells contained normal amount of ATP (30–40 nmol/mg of protein comparable with that in cardiomyocytes (about 40 nmol/mg of protein). The ATP content was decreased by half (Fig. 3B) after inhibition of glycolysis by 2-deoxyglucose. Glucose consumption and lactate production measurements performed in supernatants from cells cultured in normal medium showed effective conversion of glucose into lactate: the lactate production/glucose consumption ratio was 1.84±0.04 (n=5) (Fig. 3C), it did not depend on incubation time and was very close to the maximum value of 2 molecules of lactate per molecule of glucose consumed. These results together with the enzyme profiles described above show that NB HL-1 cells display a glycolytic phenotype of energy metabolism.

RT-PCR reaction analysis revealed expression of genes *AK2* and *CKMT* encoding mitochondrial AK and CK isoforms, respectively, and genes *AK1*, *CKM* and *CKB* encoding cytosolic isoforms of AK and CK, respectively, in the HL-1 cells. The *HK1* and *HK2* genes were also expressed, whereas expression of *HK3* gene was not detected (Fig. 4A, B). When the data were normalized to corresponding gene activities in mouse ventricular myocardium, low mRNA levels were found for *CKM*, *CKMT2* and *AK1*, whereas *AK2*, *CKB*, *HK1* and *HK2* expressed at higher levels, close to those in ventricular myocardium (Fig. 4C). Fig. 4C also shows that by transcriptional activities of the genes the B and NB HL-1 cells were similar, except that *CKM* gene expression was not as low in B as in NB cells. Fig. 5 depicts the expression of the enzyme isoforms at the protein (Fig. 5A) and activity levels (Fig. 5B, C). Since the B and NB HL-1 cells showed similar isoform profiles (results not shown) the data here are given for NB HL-1 cells only. It can be seen that the HL-1 cells contain AK1, AK2, mitochondrial CK and B-CK proteins and that the expression of mitochondrial CK and MM-CK encoded by *CKMT2* and *CKM* genes, respectively, was not detectable in a native electrophoresis of the HL-1 cell homogenates, which is probably due to a little transcriptional activity. It is also remarkable (Fig. 5B) that while in adult cardiac cells the MM-CK represents the major cytosolic CK isoform, it is totally replaced by BB-CK isoform in the cytosol of the HL-1 cells. Native electrophoresis (Fig. 5C) confirms the data obtained by real-time RT-PCR in that the HL-1 cells express HK1 and HK2 isoforms but not the HK3 isoforms, and that this profile of HK expression is similar to that in adult ventricular myocardium [25].

To assess the role of mitochondrial kinases in HL-1 cells, the presence of functional coupling between ANT and mi-AK2 or mi-CK known to exist in adult cardiomyocytes [10] was first investigated. In one set of experiments, the cells were permeabilized in oxygraph chamber followed by addition of 0.1 mM of MgATP, which caused a small stimulation of respiration due to limited amount of MgADP produced by CaMgATPases (Fig. 6A). Then 2 mM AMP was added which strongly activated respiration to 150% over basal level with MgATP. This change was fully abolished by addition of AP_5A, an inhibitor of AK, confirming that stimulation of respiration by AMP was indeed related to AK producing excess ADP from available AMP and ATP. Compared to AMP effects, creatine exerted a small but insignificant activation of respiration while added after AP_5A (Fig. 6A, B). Another set of experiments was performed to ascertain whether the activation of respiration by AMP or creatine was due to local production of ADP by mi-AK2 or mi-CK, respectively, in the space between mitochondrial inner and outer membranes, or to ADP generated by the kinases in the bulk phase of cytoplasm (Fig. 7). Fig. 7A shows a typical experiment for isolated and permeabilized cardiomyocytes from adult rat heart. First, the OXPHOS was activated by 2 mM MgATP through generation of MgADP by ATPases. Then the PK in activity of 20 IU/ml sufficient to trap all ADP available in the bulk phase of the cytoplasm [9] was added. It can be seen that PK+PEP system suppressed the overall MgADP flux to mitochondria not more than by 30–40%, which corresponds to an

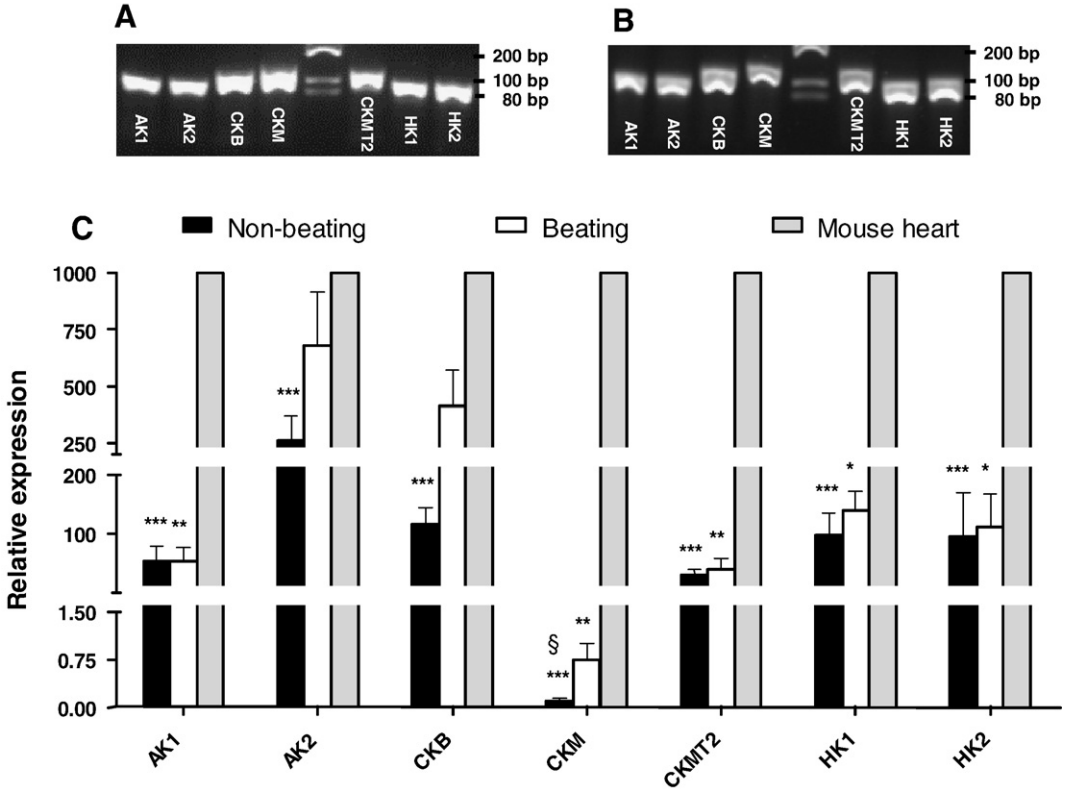

Fig. 4. 1.7% agarose gel electrophoresis of the products (amplicons) of RT-PCR amplified by gene specific primers (shown in Table 1) from the ss cDNA of B (A) and NB (B) HL-1 cells. As a result, PCR fragments of foreseeable length separated, demonstrating the expression of the transcripts of AK, CK and HK genes in HL-1 cells. DNA size marker was loaded onto the fifth lane. C. 1000-fold scaled mRNA levels of AK1, AK2, CKB, CKM, CKMT2, HK1 and HK2 in B and NB HL1 cells detected by real-time PCR relative to the expression of corresponding genes in mouse heart. n=5–14 experiments are shown. *, **, *** — $p<0.05$, $p<0.01$ or $p<0.001$, respectively, compared to corresponding mRNA level in mouse heart. § — $p<0.05$ compared to corresponding mRNA in B HL-1 cells.

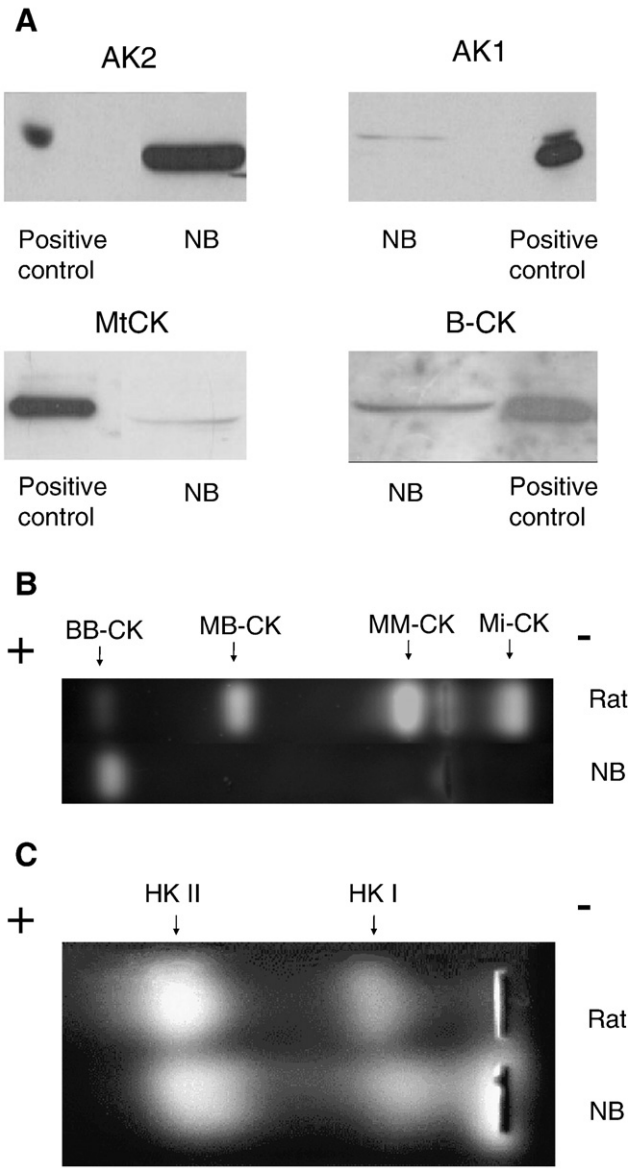

Fig. 5. A. Immunoblots tested with polyclonal rabbit antibodies against AK1, AK2, MtCK and affinity-purified chicken IgY antibodies against B-CK. Homogenized NB HL-1 cells containing 50 μg total protein were used as a sample (NB). To verify B-CK and MtCK, recombinant human proteins (approximately 1 μg) expressed in *E. coli* were applied as positive controls. For AKs, protein from the cytosolic or mitochondrial fractions of the rat heart was used as positive controls for AK1 or AK2, respectively. B. Agarose gel electrophoresis of CK isoforms. Homogenate of NB HL-1 cells was used as a sample (40 μg total protein) (NB). For control, a sample of the homogenate of rat ventricular myocardium (10 μg total protein) was run (Rat). C. Agarose gel electrophoresis of HK isoforms. Homogenate of NB HL-1 cells was used as a sample (20 μg total protein) (NB). For control, a sample of the homogenate of rat ventricular myocardium (95 μg total protein) was run (Rat).

extent of inhibition usually found in the skinned cardiomyocytes or cardiac fibers [26]. A subsequent addition of 20 mM creatine markedly stimulated respiration which is explained by accumulation of local ADP near ANT due to its functional coupling to mi-CK and ANT [26,27]. Fig. 7B shows that differently from that in cardiomyocytes, in NB HL-1 cells the PK+PEP system entirely abolished the mitochondrial activation caused by MgATP, hence the PK+PEP system fully utilized MgADP produced by CaMgATPases. In this situation creatine was unable to significantly stimulate respiration (Fig. 7B, C), whereas AMP could still produce contrastingly large activation (Fig. 7D). Thus, it was not mi-CK but mit-AK2 isoform that was coupled to OXPHOS because only the latter enzyme could increase local MgADP in the intermembrane space not available to exogenous ADP-trapping system. It is also noteworthy that MgATP at 2 mM concentration (Fig. 7B–D) did not cause larger than [MgATP] at 0.1 mM respiratory activation (Fig. 6). It means that already a very low amount of MgADP provided by MgATPases at [MgATP] of 0.1 mM was sufficient to saturate the mitochondria, suggesting high affinity of mitochondria to ADP in HL-1 cells. Indeed, our previous study has shown that the apparent Km value for ADP in regulation of OXPHOS in permeabilized HL-1 cells is much less (20–40 μM) than in permeabilized cardiomyocytes (300–400 μM) [12].

Since it has been proposed that HK protein binds to porin protein of the voltage dependent anion channel (VDAC) in the mitochondrial outer membrane (MOM) [28], we also investigated interaction of HK and OXPHOS in HL-1 cells. Interestingly, glucose exerted a marked stimulatory effect on mitochondrial respiration at 0.1 mM MgATP in both B and NB HL-1 cells, whereas its effect was negligible in permeabilized cardiomyocytes (Fig. 8). Conceivably, high level of HK1 and HK2 expression was associated with binding either one or both isoforms with VDAC in the MOM that allowed the HK to exert control over OXPHOS so that it used mitochondrially produced ATP for glucose phosphorylation and provided ADP to stimulate OXPHOS.

Fig. 9 demonstrates the results of the experiments performed to test a direct ADP transfer of adenine nucleotides between the CaMgATPases and mitochondria shown to exist in rodent and human myocardial cells [8–10]. As the first step, the CaMgATPases were activated by addition of 2 mM MgATP (Fig. 9A–C). In the absence of OXPHOS the ADP flux produced by CaMgATPases entirely passed through the PK reaction that also clamped the [ATP] in the medium. In normal cardiomyocytes (Fig. 9A, C, E), the following launching of OXPHOS by glutamate+malate resulted in significantly decreased (by 34%) ADP flux because now the endogenous ADP was partially taken up and phosphorylated by mitochondria in an atractyloside-sensitive manner, thus bypassing the route through PK. This finding means that about 34% of total MgADP produced by CaMgATPases was transferred directly to mitochondria, in agreement with previous experiments [9,12]. However, in HL-1 NB and B cells the mitochondria were unable to compete with PK+PEP system for MgADP liberated from CaMgATPase reactions; so, there was no direct transfer of ADP/ATP between mitochondria and CaMgATPases in these cells (Fig. 9B, C, E). To exclude the possibility that low activity of OXPHOS

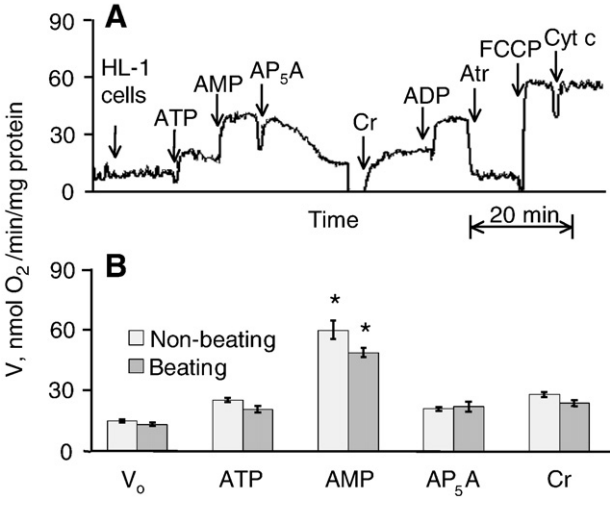

Fig. 6. Oxygraphic analysis of coupling of mitochondrial CK and AK2 to OXPHOS in HL-1 cells. A. Original recording for NB HL-1 cells. Additions: HL-1 cells — HL-1 cells incubated for 15 min in Mitomed medium at 25 °C in the presence of 50 μg/ml saponin, 10 mM succinate and 10 μM rotenone, ATP — 0.1 mM MgATP, AMP — 2 mM AMP, AP_5A — 0.2 mM diadenosine pentaphosphate, Cr — 20 mM creatine, ADP — 2 mM MgADP, Atr — 0.1 mM atractyloside, FCCP — 200 nM FCCP, Cyt *c* — 8 μM cytochrome *c*. B. The averages of measurements of respiratory parameters in comparison between B ($n=10$) and NB ($n=8$) HL-1 cells. V_0 — basal respiration rate before addition of MgATP * — $p<0.01$ as compared to respiration rate before 2 mM AMP addition.

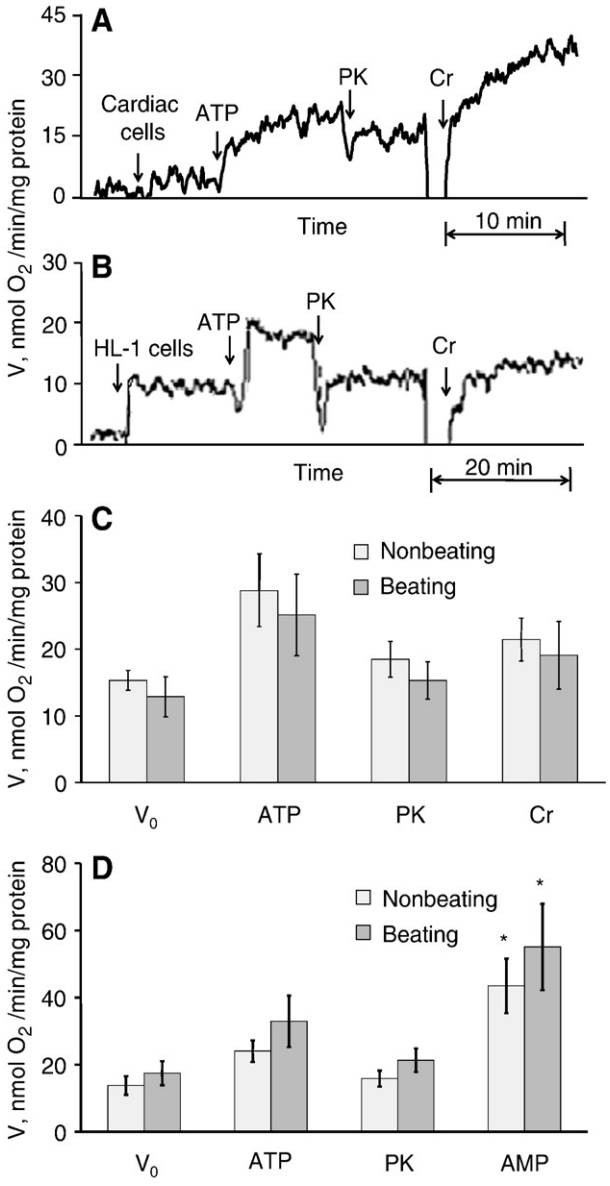

Fig. 7. Oxygraphic analysis of stimulation of OXPHOS by mitochondrial kinases via local ADP production. A. Original recording for assessing the effects of creatine on OXPHOS in saponin-permeabilized cardiomyocytes isolated from rat ventricle. The cardiomyocytes were permeabilized with 50 μg/ml saponin as shown in Materials and methods before transferring to oxygraph's chamber. After registration of the baseline respiration rate the following additions were made: ATP — 2 mM MgATP, PK — 20 IU/ml PK, Cr — 20 mM creatine. B. Original recording for assessing the effects of creatine on OXPHOS in permeabilized B HL-1 cells. The HL-1 cells were incubated with saponin as shown in the legend of Fig. 6, but in the presence of 5 mM PEP. C and D. The averages of measurements of respiratory rates of the experiments for testing the local ADP production by mitochondrial CK and AK2, respectively, in B (n=5) and NB (n=4) HL-1 cells. Additions in D are similar to that in B and C except that 2 mM AMP was added after stabilization of respiration with PK. V_0 basal respiration of HL-1 cells incubated in Mitomed medium with 5 mM PEP. * — $p<0.05$ as compared to respiration rate before 2 mM AMP addition.

due to relative deficiency of complex I of the respiratory chain could limit mitochondrial capacity to compete with PK+PEP system in HL-1 cells, the same experiments were repeated in the presence of 10 mM succinate with 10 μM rotenone, i.e. in conditions that generate much higher rates of OXPHOS than with glutamate and malate (Table 2). Again, however, the direct transfer could not be detected (results not shown), which means that the lack of it could not be related to peculiarities of the substrate-dependency of OXPHOS in these cells.

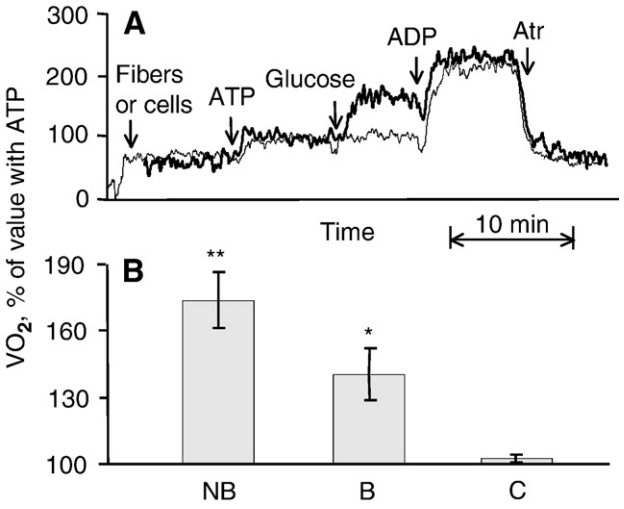

Fig. 8. Oxygraphic analysis of coupling of HK to OXPHOS in permeabilized HL-1 cells and rat ventricular cardiomyocytes. A. Original recording. Additions: ATP — 0.1 mM MgATP, Glucose — 10 mM glucose, ADP — 2 mM MgADP, Atr — 0.1 mM atractyloside. Thin line — permeabilized rat ventricular fibers; thick line — B HL-1 cells. B. The averages of stimulation of respiration in NB (n=6) and B (n=4) HL-1 cells (NB and B, respectively) and adult cardiomyocytes (C) relative to respiration rate with 0.1 mM MgATP. * — $p<0.01$; ** — $p<0.001$ compared to cardiac fibers.

It is well known that the CK-MM isoform is coupled to peripheral ATPases to regenerate local ATP near ATPases such as Ca^{2+}-ATPase in SR, myosin-ATPase in sarcomeres and Na^+-K^+-ATPase in sarcolemma

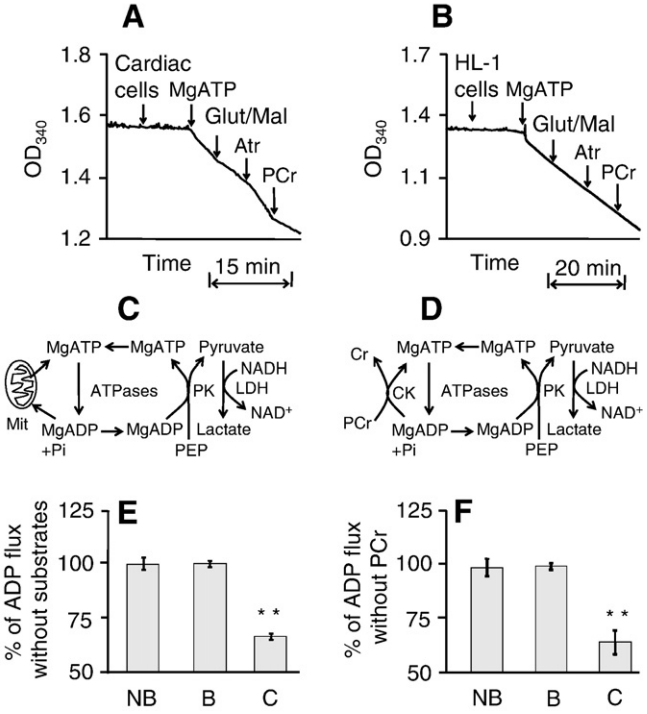

Fig. 9. A and B. Original recordings demonstrating direct transfer of ADP from ATPases to mitochondria and coupling of MM-CK to CaMgATPases in permeabilized cardiomyocytes isolated from rat ventricle and NB HL-1 cells, respectively. C and D. Reaction schemes in the spectrophotometric cuvette. Additions: Cells — 0.01–0.03 mg protein/ml (100,000–300,000 cells/ml), MgATP — 2 mM MgATP, Glut/Mal — 10 mM glutamate+2 mM malate, Atr — 0.1 mM atractyloside, PCr — 20 mM PCr. E. Absence of direct transfer of endogenous ADP from ATPases to mitochondria in HL-1 cells. The columns demonstrate the averages of the measurements in different groups. NB — NB HL-1 cells, n=4, B — B HL-1 cells, n=6, C — rat cardiomyocytes as control, n=3. ** — $p<0.005$ as compared to NB or B HL-1 groups. F. Lack of coupling of CK to ATPases to in HL-1 cells. The columns demonstrate the averages of the measurements in different groups. NB — NB HL-1 cells, n=3, B — B HL-1 cells, n=4, C — rat cardiomyocytes as control, n=3. ** — $p<0.005$ as compared to NB or B HL-1 groups.

[29–31]. In our study this coupling was assessed as a continuation of the same experiment and on the same sample used to evaluate the direct adenine nucleotide transfer. To this end, 20 mM PCr was added after atractyloside (Fig. 9A, B, D) and the effect on ADP flux available for PK+PEP system was compared with that before PCr addition. Fig. 9A and F demonstrates strong coupling of MM-CK to CaMgATPases in permeabilized cardiomyocytes, as similarly to earlier studies [29,30] PCr markedly attenuated the ADP flux (by 37%), which means that this portion of ADP generated by ATPases became unaccessible for exogenous PK+PEP system for it was rephosphorylated at the expense of PCr within the complex between MM-CK and CaMgATPases. In contrast, in HL-1 cells addition of PCr exerted no effect on ADP flux carried through the PK+PEP system, which shows that the B-CK although abundantly expressed was not coupled to CaMgATPases (Fig. 9B, F).

4. Discussion

This study features several novel and important differences in energy metabolism of cultured HL-1 cardiac cells as compared to normal cardiomyocytes. It was found that HL-1 cells display a glycolytic phenotype and possess mitochondria with deficient respiratory chain complex I. The latter conclusion stems from the observation that in state 3 the V_{Succ} markedly exceeded the V_{Glut} causing a low V_{Glut}/V_{Succ}. This index is especially sensitive to alterations in complex I because (i) being measured for each individual sample it excludes the preparation dependent variability and because (ii) it correlates with the activity ratio of complex I+III/complex II+III in many tissues [21]. In most cell types, the V_{Glut} is higher than V_{Succ}, e.g. in human atrial myocardium it equals to 1.2 [10,21]. Muscle diseases are associated with decreased V_{Glut}/V_{Succ} and this change is used to diagnose the insufficiency of complex I of the respiratory chain [21,22]. Interestingly, the V_{Succ}/V_{COX} was significantly higher in NB than in B HL-1 cells, which means that deficiency in complex I may vary between these two cell lines depending on their contractile activity.

In a recent paper, we have demonstrated an absence of coupling of mi-CK to ANT in NB HL-1 cells [12]. The present study shows that the same holds for B HL-1 cells. For both types of cells, a very low level of mi-CK expression (Fig. 4) associated with its negligible functional activity (Fig. 5) may be one reason for missed coupling, as not enough mi-CK is available for interacting with ANT at the outer aspect of mitochondrial inner membrane. Furthermore, it is obvious that although the HL-1 cells possess large amounts of BB-CK (Figs. 4 and 5), this isoform is unable to replace mi-CK for regulating OXPHOS, most likely because it cannot penetrate the MOM. This finding once again emphasizes the unique role of mi-CK in ensuring compartmentalized interaction with ANT.

A remarkable observation is that the BB-CK is not functionally coupled to CaMgATPases in HL-1 cells either. This became clear from the experiments in which the effect of exogenous PCr on ADP flux generated by CaMgATPases was monitored. In normal cardiac muscle cells, PCr strongly attenuates this flux because it triggers phosphorylation of ADP by MM-CK in a microcompartment between the CK and ATPases not accessible to exogenous PK [10,30]. For such interaction, the structural closeness of MM-CK to CaMgATPases is required, like it occurs in sarcomeres where the CK is attached to the M-line near myosin heads [32]. In other types of cells (e.g. HELA cells [33] or gastric parietal cells [34]) the BB-CK is also functionally coupled to energy consuming processes. The reason for lacking functional coupling between the BB-CK and CaMgATPases in HL-1 cells is presently unclear. Considering that in our experiments the cellular CK activity in direction of ATP formation equaled approximately to CaMgATPase measured in the same conditions (Fig. 3) and that BB-CK constitutes most of that activity (Figs. 4 and 5) it is unlikely that coupling failed due to insufficient quantity of BB-CK. More plausibly, the BB-CK, although expressed, remains unbound to specific sites near individual ATPases that hinders interaction between these two enzymes. Altogether, the current data can be taken to indicate that the CK-mediated energy transfer is not operative in HL-1 cells.

It has been proposed that whenever the intracellular CK-mediated energy transfer becomes compromised the AK-mediated system takes on a role of shuttling the energy-rich phosphoryls from mitochondria and ATPases in cardiac cells [35,36]. In that context, strong expression of mi-AK2 isoform associated with its effective control over OXPHOS (Figs. 6 and 7) may represent a compensation for inadequate mi-CK in HL-1 cells. However, it is yet uncertain whether AK system has a sufficient capacity for linking mitochondria and ATPases to each other, because the expression of cytosolic AK1 responsible for the regeneration of ATP in the vicinity of ATPases was much lower compared to mi-AK2 isoform that might limit the effectiveness of energy transfer via AK system.

We found that glucose strongly activated respiration of permeabilized HL-1 cells in the presence of exogenous ATP (Fig. 8). Several facts suggest that this phenomenon stems from specific interaction of HK isoforms with mitochondria. (i) Both HK1 and HK2 isoforms can bind to VDAC (porin) protein in the MOM in skeletal muscles and myocardium [28,37]. As a result, mitochondrially produced ATP can be used to phosphorylate glucose, whereas ADP liberated by HK reaction can be transferred back into the matrix to stimulate OXPHOS via porin connected to ANT [38–40]. (ii) We found that after permeabilization of the cell membrane, the NB and B HL-1 cells still retained the HK in activities of 197.7±52.2 (n=4) and 112.8±4.3 (n=6) nmol/min/mg of protein ($p<0.05$), respectively, which were very close to their counterparts registered in whole cell homogenates (Fig. 2). On the other hand, Parra et al. have shown that in permeabilized skeletal muscle cells all the detectable HK activity belongs to the enzyme bound to mitochondria [37]. This evidence suggests that most of the cellular HK activity remained with mitochondria in permeabilized HL-1 cells. In support of that the higher HK activity in NB cells compared to B cells correlated with stronger stimulation of respiration in former cells (Fig. 8). (iii) In our hands 30 to 70% stimulation of respiration with glucose was achieved in the presence of 0.1 mM MgATP, this concentration being far below the Km of HK for that nucleotide (0.5–1 mM [40]). In these conditions strong activation of respiration can be explained only by formation of complexes between mitochondria and HK that leads to endogenous ATP/ADP cycling thereby amplifying the respiratory response in spite of the presence of minute quantities of MgATP [40]. (iv) Overexpression of HK2 isoform and its binding to mitochondria is a characteristic feature of tumor cells [41,42]. Considering that the HL-1 cells are immortal akin to the tumor cells and that both are capable of unlimited proliferation, these cells might share other characteristics like strong expression of HK and its coupling to OXPHOS as well.

Interaction of HK with mitochondria observed in this study may represent a key step of the HK-mediated energy transfer in HL-1 cells, because it promotes glycolysis that in turn provides ATP (e.g. from PK reaction) for ATPases and ATP-dependent ion channels [31]. This assumption is substantiated further by the observations that in muscle cells coupling of HK to OXPHOS increases with enhanced workload [37] and augments the capacity of glucose uptake [28], and that the unidirectional flux of high-energy phosphoryls through glycolytic system can reach the rates equal to those of OXPHOS in muscle cells (reviewed by Dzeja and Terzic [31]).

The differences in energy metabolism between the cardiomyocytes and HL-1 cells described above might be directly related to distinct structural organization of these cells. In adult cardiomyocytes the mitochondria are tightly associated with adjacent sarcomeres into ICEUs arranged by cytoskeletal proteins, e.g. by desmin that cross-links the sarcomeres of neighboring myofilaments into register [43]. The cytoskeletal proteins also form barriers for adenine nucleotide diffusion at the level of MOM and within the ICEUS, which results in much higher apparent Km [200–400 μM] for exogenous ADP in regulation of OXPHOS in permeabilized cardiomyocytes than in isolated mitochondria [5,9,28,29,43]. To overcome diffusion limitations the ICEUs are equipped with a diversity of means of energy and feedback signal transfer — the systems mediated by different isoforms of CK and AK and direct

channeling of adenine nucleotides, which activate ATPases and OXPHOS by increasing local ATP and ADP, respectively [5,9,10,27–31]]. In contrast, in HL-1 cells where mitochondria are randomly arranged, move slowly and form dynamically changing filaments [13–15], the regulation of OXPHOS is entirely different: the Km for exogenous ADP is much lower (20–40 μM) than in cardiomyocytes [12] and exogenous PK+PEP system can easily reach the sites of ADP formation and therefore to phosphorylate it before it diffuses to mitochondria (Fig. 7). Interestingly, similar to HL-1 cells low Km for ADP can be achieved after mild treatment of cardiomyocytes with trypsin that modifies the proteins controlling diffusion of adenine nucleotides [5]. High affinity of mitochondria for ADP in regulation of respiration is also characteristic of rat permeabilized cardiomyocytes in their early postnatal stage (1–2 days after birth) when the mitochondria are still irregularly localized in the cytoplasm, mi-CK is not expressed, and sarcomeres are scarcely formed [44]. It is only during later phases of postnatal development (up to 6 weeks) that the affinity of mitochondria to exogenous ADP in these cells decreases along with increases in mi-CK expression, its functional coupling to ANT and maturation of ICEUs to the extent and quality required for normal function of adult cardiomyocytes [44]. Altogether these findings suggest that in the HL-1 cells the intracellular energy metabolism has been regressed from the ICEU-type of organization towards less developed immature system characterized by the absence of complexes formed by mitochondria and CaMgATPases and a shift from predominantly CK- to AK- and HK-mediated system of energy transfer and feedback. This type of remodeling of energy metabolism might favour the life of HL-1 cells by various means. Binding of HK enables taking advantage of mitochondria by impelling them to provide ATP for glucose phosphorylation that boosts glycolysis [28] to become a preferable energy source even in normoxic state (Fig. 3). HK also promotes VDAC closure and blocks the mitochondrial Ca^{2+}-dependent opening of the mitochondrial permeability transition pore (PTP), in association with protecting the cells from entering apoptosis [45–47]. In the context of the cellular defense mechanisms, the role of mitochondrial kinases in limiting ROS production should be taken into account. It has been recently demonstrated in brain mitochondria that the coupling of mitochondrial HK or CK isoforms to OXPHOS decreases the rate of ROS production through diminishing $\Delta\psi$ due to increased ADP recycling [48,49]. In our experiments the HL-1 cells exhibited relative insufficiency of complex I, which might give rise to excess ROS production due to attenuation of the electron flow at this step of the respiratory chain [50]. Interactions of HK and AK2 with OXPHOS might help to overcome this unfavourable situation by tuning $\Delta\psi$ to the levels associated with minimal ROS generation. Thus, it is conceivable that AK2- and HK-mediated control over mitochondrial function serves as a powerful mechanism to protect the HL-1 cells from Ca^{2+}- or ROS-induced apoptotic death, this, among other factors, giving them immortality. Further studies are required to test these hypotheses in HL-1 cells.

Acknowledgements

This work was supported by grants from Estonian Science Foundation Nos 7117 and 6142 and by grants SF 0182549As03 and SF 0180114As08 from Estonian Ministry of Education and Research, and by grant from Agence Nationale de la Recherche, France, project ANR-07-BLAN-0086-01. The authors thank E. Gvozdkova for the technical assistance and Y. Tourneur and M. Ovize, Laboratory of Cardioprotection, INSERM U886, Univ Lyon1, France for their support in carrying out this work and for their active participation in the discussion of the results.

References

[1] M. Vendelin, N. Beraud, K. Guerrero, T. Andrienko, A.V. Kuznetsov, J. Olivares, V. Saks, Mitochondrial regular arrangement in muscle cells: a “crystal-like” pattern, Am. J. Physiol. Cell Physiol. 288 (2005) C757–C767.

[2] T. Nozaki, Y. Kagaya, N. Ishide, S. Kitada, M. Miura, J. Nawata, I. Ohno, J. Watanabe, K. Shirato, Interaction between sarcomere and mitochondrial length in normoxic and hypoxic rat ventricular papillary muscles, Cardiovasc. Pathol. 10 (2001) 125–132.

[3] V.I. Veksler, A.V. Kuznetsov, K. Anflous, P. Mateo, J. van Deursen, B. Wieringa, R. Ventura-Clapier, Muscle creatine kinase deficient mice. 2. Cardiac and skeletal muscles exhibit tissue-specific adaptation of the mitochondrial function, J. Biol. Chem. 270 (1995) 19921–19929.

[4] A.V. Kuznetsov, T. Tiivel, P. Sikk, T. Kaambre, L. Kay, Z. Daneshrad, A. Rossi, L. Kadaja, N. Peet, E. Seppet, V.A. Saks, Striking differences between the kinetics of regulation of respiration by ADP in slow-twitch and fast-twitch muscles in vivo, Eur. J. Biochem. 241 (1996) 909–915.

[5] V.A. Saks, T. Kaambre, P. Sikk, M. Eimre, E. Orlova, K. Paju, A. Piirsoo, F. Appaix, L. Kay, V. Regitz-Zagrosek, E. Fleck, E. Seppet, Intracellular energetic units in red muscle cells, Biochem. J. 356 (2001) 643–657.

[6] T. Anmann, M. Eimre, A.V. Kuznetsov, T. Andrienko, T. Kaambre, P. Sikk, E. Seppet, T. Tiivel, M. Vendelin, E. Seppet, V.A. Saks, Calcium-induced contraction of sarcomeres changes the regulation of mitochondrial respiration in permeabilized cardiac cells, FEBS J. 272 (2005) 3145–3161.

[7] L. Kay, Z. Li, M. Mericskay, J. Olivares, L. Tranqui, E. Fontaine, T. Tiivel, P. Sikk, T. Kaambre, J.L. Samuel, L. Rappaport, Y. Usson, X. Leverve, D. Paulin, V.A. Saks, Study of regulation of mitochondrial respiration in vivo. An analysis of influence of ADP diffusion and possible role of cytoskeleton, Biochim. Biophys. Acta. 10 (1997) 41–59.

[8] U. Braun, K. Paju, M. Eimre, E. Seppet, E. Orlova, L. Kadaja, S. Trumbeckaite, F.N. Gellerich, S. Zierz, H. Jockusch, E.K. Seppet, Lack of dystrophin is associated with altered integration of the mitochondria and ATPases in slow-twitch muscle cells of MDX mice, Biochim. Biophys. Acta 1505 (2001) 258–270.

[9] E.K. Seppet, T. Kaambre, P. Sikk, T. Tiivel, H. Vija, M. Tonkonogi, K. Sahlin, L. Kay, F. Appaix, U. Braun, M. Eimre, V.A. Saks, Functional complexes of mitochondria with Ca,MgATPases of myofibrils and sarcoplasmic reticulum in muscle cells, Biochim. Biophys. Acta 1504 (2001) 379–395.

[10] E. Seppet, M. Eimre, N. Peet, K. Paju, E. Orlova, M. Ress, S. Kovask, A. Piirsoo, V.A. Saks, F.N. Gellerich, S. Zierz, E.K. Seppet, Compartmentation of energy metabolism in atrial myocardium of patients undergoing cardiac surgery, Mol. Cell. Biochem. 270 (2005) 49–61.

[11] M. Vendelin, M. Eimre, E. Seppet, N. Peet, T. Andrienko, M. Lemba, J. Engelbrecht, E.K. Seppet, V.A. Saks, Intracellular diffusion of adenosine phosphates is locally restricted in cardiac muscle, Mol. Cell. Biochem. 256/257 (2004) 229–241.

[12] T. Anmann, R. Guzun, N. Beraud, S. Pelloux, A.V. Kuznetsov, L. Kogerman, T. Kaambre, P. Sikk, K. Paju, N. Peet, E. Seppet, C. Ojeda, Y. Tourneur, V. Saks, Different kinetics of the regulation of respiration in permeabilized cardiomyocytes and in HL-1 cardiac cells. Importance of cell structure/organization for respiration regulation, Biochim. Biophys. Acta 1757 (2006) 1597–1606.

[13] W.C. Claycomb, N.A. Lanson Jr., B.S. Stallworth, D.B. Egeland, J.B. Delcarpio, A. Bahinski, N.J. Izzo Jr., HL-1 cells: a cardiac muscle cell line that contracts and retains phenotypic characteristics of the adult cardiomyocyte, Proc. Nat. Acad. Sci. U. S. A. 95 (1998) 2979–2984.

[14] S.M. White, P.E. Constantin, W.C. Claycomb, Cardiac physiology at the cellular level: use of cultured HL-1 cardiomyocytes for studies of cardiac muscle cell structure and function, Am. J. Physiol. Heart Circ. Physiol. 286 (2004) H823–H829.

[15] S. Pelloux, J. Robillard, R. Ferrera, A. Bilbaut, C. Ojeda, V. Saks, M. Ovize, Y. Tourneur, Non-beating HL-1 cells for confocal microscopy: application to mitochondrial functions during cardiac preconditioning, Progr. Biophys. Mol. Biol. 90 (2006) 270–298.

[16] E. Seppet, M. Eimre, K. Paju, L. Kadaja, E. Orlova, Energy transfer in cardiac cells: structure-function relationships, J. Mol. Cell. Cardiol. 42 (2007) S69.

[17] V.A. Saks, V.I. Veksler, A.V. Kuznetsov, L. Kay, P. Sikk, T. Tiivel, L. Tranqui, J. Olivares, K. Winkler, F. Wiedemann, W.S. Kunz, Permeabilized cell and skinned fiber techniques in studies of mitochondrial function in vivo, Mol. Cell. Biochem. 184 (1998) 81–100.

[18] E. Gnaiger, A.V. Kuznetsov, S. Schneeberger, R. Seiler, G. Brandacher, W. Steurer, R. Margreiter, Mitochondria in the cold, in: G. Heldmaier, M. Klingenspor (Eds.), Life in the Cold, Springer, Heidelberg, 2000, pp. 431–442.

[19] U. Schlattner, N. Möckli, O. Speer, S. Werner, T. Wallimann, Creatine kinase and creatine transporter in normal, wounded and diseased skin, J. Invest. Dermatol. 118 (2002) 416–423.

[20] K.J. Livak, T.D. Schmittgen, Analysis of relative gene expression data using real-time quantitative PCR and the $2^{-\Delta\Delta C_T}$ method, Methods 25 (2001) 402–408.

[21] E. Seppet, Z. Gizatullina, S. Trumbeckaite, S. Zierz, F. Striggow, F.N. Gellerich, Mitochondrial medicine: the central role of cellular energetic depression and mitochondria in cell pathophysiology, in: V. Saks (Ed.), Molecular System Bioenergetics: Energy for Life, WILEY-VCH Verlag GmbH & Co. KGaA, Weinheim, 2007, pp. 479–520.

[22] F.N. Gellerich, M. Deschauer, Y. Chen, T. Müller, S. Neudecker, S. Zierz, Functional impairment of mitochondria in skinned fibers of CPEO patients with single and multiple deletions of mt-DNA correlate with heteroplasmy, Biochim. Biophys. Acta 1556 (2002) 41–52.

[23] C. Vannier, V. Veksler, H. Mekhfi, P. Mateo, R. Ventura-Clapier, Functional tissue and developmental specificities of myofibrils and mitochondria in cardiac muscle, Can. J. Physiol. Pharmacol. 74 (1996) 23–31.

[24] K. Anflous, V. Veksler, P. Mateo, F. Samson, V. Saks, R. Ventura-Clapier, Mitochondrial creatine kinase isoform expression does not correlate with its mode of action, Biochem. J. 322 (1997) 73–78.

[25] H.M. Katzen, T.T. Schimke, Multiple forms of hexokinase in the rat: tissue distribution, age dependency, and properties, Proc. Natl. Acad. Sci. U. S. A. 54 (1965) 218–225.

[26] T. Andrienko, A.V. Kuznetsov, T. Käämbre, Y. Usson, A. Orosco, F. Appaix, T. Tiivel, P. Sikk, M. Vendelin, R. Margreiter, V.A. Saks, Metabolic consequences of functional complexes of mitochondria, myofibrils and sarcoplasmic reticulum in muscle cells, J. Exp. Biol. 206 (2003) 2059–2072.

[27] V.A. Saks, A.V. Kuznetsov, M. Vendelin, K. Guerrero, L. Kay, E.K. Seppet, Functional coupling as a basic mechanism of feedback regulation of cardiac energy metabolism, Mol. Cell. Biochem. 256/257 (2004) 185–199.
[28] K. Anflous-Pharayra, Z.-J. Cai, W.J. Craigen, VDAC1 serves as a mitochondrial binding site for hexokinase in oxidative muscles, Biochim. Biophys. Acta 1767 (2007) 136–142.
[29] V. Saks, K. Guerrero, M. Vendelin, J. Engelbrecht, E. Seppet, The creatine kinase isoenzymes in organized metabolic networks and regulation of cellular respiration: a new role for Maxwell's demon, in: C. Vial, V.N. Uversky (Eds.), Creatine Kinase, series Ed., Molecular Anatomy and Physiology of Proteins, NovaScience Publishers, New York, 2006, pp. 223–267.
[30] V.A. Saks, R. Ventura-Clapier, Z.A. Huchua, A.N. Preobrazhensky, I.V. Emelin, Creatine kinase in regulation of heart function and metabolism. I. Further evidence for compartmentation of adenine nucleotides in cardiac myofibrillar and sarcolemmal coupled ATPase-creatine kinase systems, Biochim. Biophys. Acta 803 (1984) 254–264.
[31] P.P. Dzeja, A. Terzic, Phosphotransfer networks and cellular energetics, J. Exp. Biol. 206 (2003) 2039–2047.
[32] T. Hornemann, M. Stolz, T. Wallimann, Isoenzyme-specific interaction of muscle-type creatine kinase with the sarcomeric M-line is mediated by NH(2)-terminal lysine charge-clamps, J. Cell Biol. 149 (2000) 1225–1234.
[33] T.S. Bürklen, A. Hirschy, T. Wallimann, Brain-type creatine kinase BB-CK interacts with the Golgi Matrix Protein GM130 in early prophase, Mol. Cell. Biochem. 297 (2007) 53–64.
[34] E.A. Sistermans, C.H.W. Klaassen, W. Peters, H.G.P. Swarts, P.H.K. Jap, J.J.H.H.M. De Pont, B. Wieringa, Co-localization and functional coupling of creatine kinase B and gastric H+/K+-ATPase on the apical membrane and the tubulovesicular system of parietal cells, Biochem. J. 311 (1995) 445–451.
[35] P.P. Dzeja, R.J. Zeleznikar, N.D. Goldberg, Adenylate kinase: kinetic behavior in intact cells indicates it is integral to multiple cellular processes, Mol. Cell. Biochem. 184 (1998) 169–182.
[36] D. Pucar, E. Janssen, P.P. Dzeja, N. Juranic, S. Macura, B. Wieringa, A. Terzic, Compromised energetics in the adenylate kinase AK1 gene knockout heart under metabolic stress, J. Biol. Chem. 275 (2000) 41424–41429.
[37] J. Parra, D. Brdiczka, R. Cusso, D. Pette, Enhanced catalytic activity of hexokinase by work-induced mitochondrial binding in fast-twitch muscle of rat, FEBS Lett. 403 (1997) 279–282.
[38] Y. Shinohara, I. Sagawa, J. Ichihara, K. Yamamoto, K. Terao, H. Terada, Source of ATP for hexokinase-catalyzed glucose phosphorylation in tumor cells: dependence on the rate of oxidative phosphorylation relative to that of extramitochondrial ATP generation, Biochim. Biophys. Acta. 1319 (1997) 319–330.
[39] P.V. Viitanen, P.J. Geiger, S. Erickson-Viitanen, S.P. Bessman, Evidence of functional hexokinase compartmentation in rat skeletal muscle mitochondria, J. Biol. Chem. 259 (1984) 9679–9686.
[40] J.E. Wilson, Isozymes of mammalian hexokinase: structure, subcellular localization and metabolic function, J. Exp Biol. 206 (2003) 2049–2057.
[41] S.P. Mathupala, Y.H. Ko, P.L. Pedersen, Hexokinase II: cancer's double edged sword acting as both facilitator and gatekeeper of malignancy when bound to mitochondria, Oncogene 25 (2006) 4777–4786.
[42] G.-Y. Gwak, J.-H. Yoon, K.M. Kim, H.-S. Lee, J.W. Chung, G.J. Gores, Hypoxia stimulates proliferation of human hepatoma cells through the induction of hexokinase II expression, J. Hepatol. 42 (2005) 358–364.
[43] Y. Capetanaki, Desmin cytoskeleton: a potential regulator of muscle mitochondrial behavior and function, Trends Cardiovasc. Med. 12 (2002) 339–348.
[44] T. Tiivel, L. Kadaya, A. Kuznetsov, T. Käämbre, N. Peet, N.P. Sikk, U. Braun, R. Ventura-Clapier, V. Saks, E.K. Seppet, Developmental changes in regulation of mitochondrial respiration by ADP and creatine in rat heart in vivo, Mol. Cell. Biochem. 206 (2000) 119–128.
[45] J.G. Pastorino, N. Shulga, J.B. Hoek, Mitochondrial binding of hexokinase II inhibits Bax-induced cytochrome *c* release and apoptosis, J. Biol. Chem. 277 (2002) 7610–7618.
[46] J.M. Bryson, P.E. Coy, K. Gottlob, N. Hay, R.B. Robey, Increased hexokinase activity, of either ectopic or endogenous origin, protects renal epithelial cells against acute oxidant-induced cell death, J. Biol. Chem. 277 (2002) 11392–11400.
[47] H. Azoulay-Zohar, A. Israelson, S. Abu-Hamad, V. Shoshan-Barmatz, In self-defence: hexokinase promotes voltage-dependent anion channel closure and prevents mitochondria-mediated apoptotic cell death, Biochem. J. 377 (2004) 347–355.
[48] W.S. da-Silva, A. Gómes-Puyou, M.T. de Gómes-Puyou, R. Moreno-Sanchez, F.G. De Felice, L. de Meis, M.F. Oliveira, A. Galina, Mitochondrial bound hexokinase activity as a preventive antioxidant defence, J. Biol. Chem. 279 (2004) 39846–39855.
[49] L.E. Meyer, L.B. Machado, A.P. Santiago, W.S. da-Silva, F.G. De Felice, O. Holub, M.F. Oliveira, A. Galina, Mitochondrial creatine kinase activity prevents reactive oxygen species generation: antioxidant role of mitochondrial kinase-dependent ADP re-cycling activity, J. Biol. Chem. 281 (2006) 37361–37371.
[50] M. Brandon, P. Baldi, D.C. Wallace, Mitochondrial mutations in cancer, Oncogene 25 (2006) 4647–4662.